Molecular Cancer Therapeutics

Mitochondria-Targeted Doxorubicin: A New Therapeutic Strategy against Doxorubicin-Resistant Osteosarcoma

Ilaria Buondonno[1], Elena Gazzano[1], Sae Rin Jean[2,3], Valentina Audrito[4,5], Joanna Kopecka[1], Marilù Fanelli[6], Iris C. Salaroglio[1], Costanzo Costamagna[1], Ilaria Roato[7], Eleonora Mungo[1], Claudia M. Hattinger[6], Silvia Deaglio[4,5], Shana O. Kelley[2,3], Massimo Serra[6], and Chiara Riganti[1]

Abstract

Doxorubicin is one of the leading drugs for osteosarcoma standard chemotherapy. A total of 40% to 45% of high-grade osteosarcoma patients are unresponsive, or only partially responsive, to doxorubicin (Dox), due to the overexpression of the drug efflux transporter ABCB1/P-glycoprotein (Pgp). The aim of this work is to improve Dox-based regimens in resistant osteosarcomas. We used a chemically modified mitochondria-targeted Dox (mtDox) against Pgp-overexpressing osteosarcomas with increased resistance to Dox. Unlike Dox, mtDox accumulated at significant levels intracellularly, exerted cytotoxic activity, and induced necrotic and immunogenic cell death in Dox-resistant/Pgp-overexpressing cells, fully reproducing the activities exerted by anthracyclines in drug-sensitive tumors. mtDox reduced tumor growth and cell proliferation, increased apoptosis, primed tumor cells for recognition by the host immune system, and was less cardiotoxic than Dox in preclinical models of drug-resistant osteosarcoma. The increase in Dox resistance was paralleled by a progressive upregulation of mitochondrial metabolism. By widely modulating the expression of mitochondria-related genes, mtDox decreased mitochondrial biogenesis, the import of proteins and metabolites within mitochondria, mitochondrial metabolism, and the synthesis of ATP. These events were paralleled by increased reactive oxygen species production, mitochondrial depolarization, and mitochondria-dependent apoptosis in resistant osteosarcoma cells, where Dox was completely ineffective. We propose mtDox as a new effective agent with a safer toxicity profile compared with Dox that may be effective for the treatment of Dox-resistant/Pgp-positive osteosarcoma patients, who strongly need alternative and innovative treatment strategies.
Mol Cancer Ther; 15(11); 2640–52. ©2016 AACR.

Introduction

Osteosarcoma is the most frequent bone tumor observed clinically. The standard treatment for conventional osteosarcoma (tumors, which are not metastatic at clinical onset, with high-grade malignancy, located at the extremities in patients younger than 40 years) is based on pre- and postoperative chemotherapy, including doxorubicin (Dox), cisplatin, and methotrexate. This treatment is successful in about 55% to 60% of patients. Despite numerous attempts to find new therapeutic approaches for osteosarcoma, the patients' prognosis has not improved in the last decades (1, 2, and references therein). The main drawbacks of Dox are the onset of drug resistance that makes chemotherapy progressively ineffective (2) and the onset of cardiotoxicity (3).

Dox is a substrate of ATP-binding cassette (ABC) transporters, such as ABCB1/P-glycoprotein (Pgp) and ABCC1/multidrug resistance related protein 1 (MRP1), which efflux the drug outside the tumor cell and limit its cytotoxicity (4). The presence of Pgp in osteosarcoma patients is a negative prognostic factor and is predictive of poor response to treatment (5–8). Both natural (9, 10) and synthetic (11, 12) inhibitors of Pgp have been tested to reverse Dox resistance in osteosarcoma cell lines *in vitro*. The specific silencing of Pgp (13) or the inhibition of pathways involved in drug resistance—such as the hypoxia inducible factor-1α– (14) or polo-like kinase 1–dependent signaling (15)—appears to be promising strategies, but the translation of these approaches to clinical settings is still under investigation.

Recently, targeting mitochondria of osteosarcoma cells has been proposed as an effective therapeutic strategy (16). On the other hand, because the heart has an aerobic mitochondria-based metabolism, mitochondria-targeting drugs—while effective on tumor cells—may produce serious cardiotoxicity.

We recently developed chemically modified Dox derivatives with mitochondrial tropism that are effective against drug-resistant tumor cells overexpressing Pgp (17, 18). One of these

[1]Department of Oncology, University of Torino, Torino, Italy. [2]Department of Pharmaceutical Sciences, Leslie Dan Faculty of Pharmacy, University of Toronto, Toronto, Ontario, Canada. [3]Department of Chemistry, Faculty of Arts and Science, University of Toronto, Toronto, Ontario, Canada. [4]Human Genetics Foundation (HuGeF), Torino, Italy. [5]Department of Medical Sciences, University of Torino, Torino, Italy. [6]Orthopaedic Rizzoli Institute, Laboratory of Experimental Oncology, Pharmacogenomics and Pharmacogenetics Research Unit, Bologna, Italy. [7]Center for Research and Experimental Medicine (Ce.R.M.S.), San Giovanni Battista Hospital, Torino, Italy.

Note: Supplementary data for this article are available at Molecular Cancer Therapeutics Online (http://mct.aacrjournals.org/).

Corresponding Author: Chiara Riganti, University of Torino, via Santena 5/bis, 10126 Torino, Italy. Phone: 390116705857; Fax: 390116745845; E-mail: chiara.riganti@unito.it

doi: 10.1158/1535-7163.MCT-16-0048

mitochondria-targeted Dox compounds (mtDox; 18) did not elicit cardiotoxicity in animals, showing a safer toxicity profile compared with Dox (19).

In this work, we used mtDox against Pgp-overexpressing osteosarcomas *in vitro* and *in vivo* and found that it was significantly more effective and less cardiotoxic than Dox, and that it overcame drug resistance by exploiting the metabolic signature typical of drug-resistant osteosarcoma cells. Our data indicate mtDox as a very promising new chemotherapeutic drug for a possible clinical application in Dox-unresponsive patients.

Materials and Methods

Chemicals

FBS and culture medium were from Invitrogen Life Technologies. Plasticware for cell cultures was from Falcon (Becton Dickinson). The protein content in cell monolayers, mitochondrial, and nuclear extracts was assessed with the BCA Kit from Sigma Chemical Co. Electrophoresis reagents were obtained from Bio-Rad Laboratories. Dox was purchased by Sigma Chemical Co. mtDox (Supplementary Fig. S1) was synthesized as described in ref. 18. Unless otherwise specified, all the other reagents were purchased from Sigma Chemical Co.

Cell lines

Murine osteosarcoma K7M2 cells, human Dox-sensitive osteosarcoma U-2OS and Saos-2 cells, and rat neonatal H9c2 cardiomyocytes were purchased from the ATCC in 2012. The corresponding variants with increasing resistance to Dox (U-2OS/DX30, U-2OS/DX100, U-2OS/DX580, Saos-2/DX30, Saos-2/DX100, and Saos-2/DX580), selected by culturing parental cells in a medium with 30, 100, and 580 ng/mL Dox, were generated as reported in ref. 20. All cell lines were authenticated by microsatellite analysis, using the PowerPlex Kit (Promega Corporation; last authentication: September 2015). Mesenchymal stem cells, derived by discarded lipoaspirates of healthy subjects, were cultured in osteogenic condition to obtain primary nontransformed osteoblasts (21, 22). Fourteen days after culture, Bone Alkaline Phosphatase (BAP staining Kit; Sigma Chemicals Co.) was performed as authentication test for osteoblasts (last authentication: April 2016). Cells were maintained in medium supplemented with 10% v/v FBS, 1% v/v penicillin–streptomycin, and 1% v/v L-glutamine. Drug-resistant variants were continuously cultured in presence of Dox.

Cell viability and proliferation

Cell viability was measured by the neutral red staining method, as previously reported (23). The absorbance of untreated cells was considered as 100% viability; the results were expressed as a percentage of viable cells versus untreated cells. To determine IC_{50}, reported in Supplementary Table S1, 1×10^5 cells were incubated for 72 hours with increasing concentrations of Dox or mtDox (from 1 nmol/L to 1 mmol/L). IC_{50} was considered the concentration of the drug that reduced cell viability to 50%. Cell-cycle analysis was measured by flow cytometry, after propidium iodide staining (24).

ABCB1/Pgp and ABCC1/MRP1 expression

For flow cytometry assays, cells were harvested, washed once in PBS, twice with 10 mmol/L Hepes in Hank's balanced salt solution, and fixed with 4% paraformaldehyde in PBS for 5 minutes. After a wash in Hepes, cells were permeabilized in 0.1% w/v saponin and incubated with an anti-ABCB1/Pgp (clone MRK16; Kamiya) or anti-ABCC1/MRP1 (clone MRPm5; Abcam) antibodies. After washing with saponin, cells were incubated with a secondary anti-mouse FITC-conjugated antibody (Sigma Chemical Co.), washed twice with saponin and once with Hepes. In the negative control, primary antibody was replaced by 0.1% saponin. Samples were analyzed by flow cytometry (FACSCalibur; Becton Dickinson). For Western blot analysis, 20 μg of proteins from cell lysates were probed with anti-Pgp (clone 17F9; BD Biosciences) or anti–β-tubulin (clone D-10; Santa Cruz Biotechnology Inc.) antibodies.

Confocal microscope analysis

Cells (5×10^5) were grown on sterile glass coverslips and transfected with the GFP-E1α pyruvate dehydrogenase expression vector (Cell Light BacMan 2.0; Invitrogen Life Technologies) to label mitochondria. After 24 hours, cells were incubated with 5 μmol/L Dox or mtDox for 6 hours. Samples were rinsed with PBS, fixed with 4% w/v paraformaldehyde for 15 minutes, washed 3 times with PBS and once with water, and mounted with 4 μL of Gel Mount Aqueous Mounting. Slides were analyzed using an Olympus FV300 laser scanning confocal microscope (Olympus Biosystems; ocular lens: 10X; objective: 60X). For each experimental condition, a minimum of 5 microscopic fields were examined.

Isolation of mitochondria and nuclei

Mitochondria were isolated as reported in ref. 25. A 50 μL aliquot was sonicated and used for the measurement of protein content or Western blotting; the remaining part was stored at −80°C until use. To confirm the presence of mitochondrial proteins in the extracts, 10 μg of each sonicated sample were subjected to SDS-PAGE and probed with an anti-porin antibody (clone 20B12AF2; Abcam). To exclude any mitochondrial contamination in the cytosolic extracts, the absence of porin in the latter was analyzed by Western blotting. Nuclear proteins were extracted using the Nuclear Extract Kit (Active Motif). To exclude any cytosolic contamination in the nuclear extracts, the absence of actin (#A2066; Sigma Chemical Co.) in the latter was analyzed by Western blotting.

Dox accumulation

Cellular, nuclear, or mitochondrial extracts were resuspended in 0.5 mL ethanol/0.3 N HCl. The amount of Dox was measured fluorimetrically (17). Fluorescence was converted into nmol/mg cellular, nuclear, or mitochondrial proteins, using a previously set calibration curve.

Necrotic and immunogenic death assays

The activity of lactate dehydrogenase (LDH) released in the extracellular medium, taken as index of necrotic cell death, was measured spectrophotometrically (26). The results were expressed as the percentage of extracellular LDH activity versus total (intracellular + extracellular) LDH activity. To evaluate the immunogenic cell death induced by Dox, the extracellular release of ATP was measured by a chemiluminescence-based assay, the extracellular release of high mobility group box 1 (HMGB1) protein was measured by Western blotting. Following a procedure commonly used in the immunoblotting of extracellular proteins (27), we stained the blot with Red Ponceau and reported a band at

the same level of the HMGB1 band, as the control of equal protein loading. Surface translocation of calreticulin, detected by flow cytometry, was measured (27). The mean fluorescence intensity was calculated using Cell Quest software (Becton Dickinson).

Tumor cell phagocytosis

Murine dendritic cells (DC) were obtained as reported by Obeid and colleagues (28). Tumor cell phagocytosis was performed by flow cytometry (28). In each set of experiments, a phagocytosis assay was performed by coincubating DCs and tumor cells at 4°C, instead of 37°C, and the percentage of phagocytized cells at 4°C was subtracted from values observed at 37°C. The phagocytosis rate was expressed as a phagocytic index, calculated as previously reported (28).

In vivo tumor growth, hematochemical parameters, and immunohistochemical analysis

1×10^6 K7M2 cells, stably transfected with the pGL4.51[luc2/CMV/Neo] Vector (Promega Corporation), mixed with 100 μL Matrigel, were injected s.c. in 6-week-old female BALB/c mice (weight: 20 g ± 1.3; Charles River Laboratories Italia); 1×10^7 U-2OS cells, mixed with 100 μL Matrigel, were injected s.c. in 6-week-old female NOD SCID BALB/c mice (weight: 19.6 g ± 1.6; Charles River Laboratories Italia). Animals were housed (5 per cage) under 12-hour light/dark cycles, with food and drinking provided *ad libitum*. Tumor growth was measured daily by caliper and calculated according to the equation $(L \times W^2)/2$, where L = tumor length and W = tumor width. When the tumor reached a volume of 50 mm^3 (day 7 after injection), the mice were randomized into 3 groups: (1) Control group, treated with 0.1 mL saline solution i.v. on days 7, 14, 21, and 28; (2) Dox group, treated with Dox i.v. on days 7, 14, 21, and 28; (3) mtDox group, treated with mitochondria-targeting Dox i.v. on days 7, 14, 21, and 28. *In vivo* bioluminescence imaging was performed on days 7, 21, and 35 with a Xenogen IVIS Spectrum (PerkinElmer). Tumor volumes were monitored daily by caliper, and animals were euthanized by injecting zolazepam (0.2 mL/kg) and xylazine (16 mg/kg) i.m. at day 35. The inhibition rate was calculated as a percentage (i.e., the tumor weight of the control group minus that of the tumor weight of the test group) divided by the tumor weight of the control group. The hematochemical parameters LDH, aspartate aminotransferase (AST), alanine aminotransferase (ALT), alkaline phosphatase (AP), creatinine, creatine phosphokinase (CPK) were measured on 0.5 mL of blood collected immediately after mice sacrifice, using the respective kits from Beckman Coulter Inc. For immunohistochemical analysis, tumors were resected and fixed in 4% v/v paraformaldehyde. The paraffin sections were stained with hematoxylin/eosin or immunostained for Ki67 (AB9260; Millipore), cleaved caspase 3 (#9661, Asp175; Cell Signaling Technology Inc.), calreticulin (#PA3900; Affinity Bioreagents), CD11c (clone HL3; BD Biosciences), followed by a peroxidase-conjugated secondary antibody (Dako). Nuclei were counterstained with hematoxylin. Sections were examined with a Leica DC100 microscope (Leica Microsystems GmbH; 10× ocular lens, 20× objective).

All animal care and experimental procedures were approved by the Bio-Ethical Committee of the University of Torino, Italy.

PCR arrays and qRT-PCR

Total RNA was extracted and reverse-transcribed using the iScript cDNA Synthesis Kit (Bio-Rad Laboratories). The PCR arrays were performed on 1 μg cDNA, using Mitochondria and Mitochondria Energy Metabolism Arrays (Bio-Rad Laboratories). The expression levels of specific mitochondria-related genes, representative of the main biological categories screened by PCR arrays, were validated by qRT-PCR. Primer sequences were designed using qPrimerDepot software (https://primerdepot.nci.nih.gov/). *S14* was used as the housekeeping gene. Data analysis was performed with PrimePCR Analysis Software (Bio-Rad Laboratories).

Mitochondrial DNA quantification

Mitochondrial DNA was extracted, amplified, and quantified by PicoGreen (Invitrogen Life Technologies) staining as reported in ref. 19. The results are expressed as ng DNA/10^5 cells.

Mitochondria biogenesis

The expression of peroxisome proliferator-activated receptor gamma coactivator-1α (PGC-1α), measured on 30 μg of nuclear proteins and considered an index of increased mitochondria biogenesis (29), was evaluated by Western blotting, using an anti–PGC-1α (#ab54481; Abcam) antibody. An anti–TATA-box binding protein (TBP; clone 58C9; Santa Cruz Biotechnology Inc.) was used to check equal protein loading. Mitochondria biogenesis was also evaluated by measuring the expressions of subunit I of complex IV (COX-I), which is encoded by mitochondrial DNA, and succinate dehydrogenase-A of complex II (SDH-A), which is encoded by nuclear DNA, using the MitoBiogenesis In-Cell ELISA Kit (Abcam). The results are expressed as units (U) of each protein/mg mitochondrial proteins.

Tricarboxylic acid cycle

The glucose flux through tricarboxylic acid (TCA) cycle was measured by radiolabeling cells with 2 μCi/mL [6-^{14}C]-glucose (55 mCi/mmol; PerkinElmer). Cell suspensions were incubated for 1 hour in a closed experimental system to trap the $^{14}CO_2$ developed from [^{14}C]-glucose. The reaction was stopped by injecting 0.8 N $HClO_4$. The amount of glucose transformed into CO_2 through the TCA cycle was calculated as described by Riganti and colleagues (30) and expressed as pmol CO_2/h/mg cellular proteins.

Fatty acids β-oxidation

Long-chain fatty acids β-oxidation was measured as detailed in ref. 31. The precipitates, containing ^{14}C-acid soluble metabolites (ASM), were collected. The radioactivity of each sample was counted by liquid scintillation. Results are expressed as nmol/min/mg cellular proteins. In each experimental set, cells were preincubated for 30 minutes with the carnitine palmitoyltransferase inhibitor etomoxir (1 μmol/L) or with the AMP-kinase activator 5-aminoimidazole-4-carboxamide ribonucleotide (AICAR; 1 mmol/L), as negative and positive controls, respectively. In the presence of etoxomir, the rate of β-oxidation was less than 10% than in its absence; in the presence of AICAR, the rate of β-oxidation was increased 2-fold.

Mitochondrial energy metabolism

The oxygen consumption rate (OCR) was measured on 20,000 cells with the XFp Mito Stress Test Kit, using a Seahorse XFp Extracellular Flux Analyzer (Seahorse Bioscience, M&M Biotech). Carbonyl cyanide 4-(trifluoromethoxy) phenylhydrazone (FCCP) was used at a concentration of 0.3 μmol/L to uncouple mitochondrial oxidative phosphorylation and induce maximal

respiration. The data were analyzed using Wave Seahorse software. The amount of ATP produced by oxidative phosphorylation was measured on 20 μg mitochondrial proteins with the ATP Bioluminescent Assay Kit (FL-AA; Sigma Chemical Co.). Data were converted into nmol/mg mitochondrial proteins, using a previously set calibration curve.

Intramitochondrial reactive oxygen species levels

After extraction, mitochondria were incubated with the reactive oxygen species (ROS)–sensitive probe 5-(and-6)-chloromethyl-2′,7′-dichlorodihydro-fluorescein diacetate-acetoxymethyl ester (5 μmol/L; DCFDA-AM), as described (32).The results are expressed as nmol/mg mitochondrial proteins.

Mitochondrial electric potential ($\Delta\psi$) measurement

Staining with JC-1 fluorescent probe (Biotium Inc.) was performed (32). The fluorescence units were used to calculate the percentage of green-fluorescent (i.e., depolarized) mitochondria versus red-fluorescent (i.e., polarized) mitochondria.

Apoptosis measurement

20 μg proteins of whole cell, cytosolic, or mitochondrial extracts were subjected to the Western blot analysis with the following antibodies (all from Cell Signaling Technology): anti-BAD (clone 11E3); anti-BAK (clone D4E4); anti-BAX (#2772); anti-BID (#2002); anti-BIM (clone C34C5); anti-PUMA (clone D30C10); anti-BCL-2 (#2872); anti-BCL-xL (clone #2762); anti-cytochrome c (#4272). Images were acquired by Image Lab software (Bio-Rad Laboratories). Caspase 9 and caspase 3 activity was measured fluorimetrically in the cytosolic extracts (17).The results are expressed as nmol of the hydrolyzed substrate of each caspase/mg cellular proteins, according to a previously set titration curve.

Statistical analysis

All data in the text and figures are provided as mean ± SD. The results were analyzed by a one-way ANOVA and Tukey test. $P < 0.05$ was considered significant.

Results

Mitochondria-targeted Dox is effective against Dox-resistant osteosarcoma

We compared the antitumor efficacy of Dox and mtDox in the Dox-sensitive human osteosarcoma U-2OS cells and in the corresponding Dox-resistant variants U-2OS/DX30, U-2OS/DX100, U-2OS/DX580, with increasing expression of Pgp and MRP1 (Supplementary Fig. S2). Dox exhibited typical nuclear localization in U-2OS cells (Fig. 1A). There was a high accumulation of the drug in the nuclear extracts (Fig. 1B) and a low accumulation in mitochondria (Fig. 1C) in U-2OS cells, whereas both nuclear and mitochondrial accumulation progressively decreased in U-2OS/DX30, U-2OS/DX100, and U-2OS/DX580 cells. By contrast, mtDox had a distinct mitochondrial localization profile in U-2OS cells (Fig. 1A): intranuclear accumulation was very low in both sensitive and resistant cells (Fig. 1B); intramitochondrial accumulation was significantly higher than Dox and progressively increased in the resistant cells (Fig. 1C). At a concentration (5 μmol/L) corresponding to the IC_{50} in chemosensitive osteosarcoma (Supplementary Table S1), Dox retention in the whole cell was progressively lower (Fig. 1D), and the inhibition of cell survival was lost (Fig. 1E) in the resistant variants. However, at the same concentration, mtDox exhibited lower intracellular accumulation in the most resistant variants (Fig. 1D), but it still reduced cell survival (Fig. 1E).

Dox is one of the few chemotherapeutic drugs able to induce direct cytotoxicity on tumor cells, as indicated by the extracellular release of LDH (26), and to elicit tumor immunogenic cell death, typically followed by tracking the extracellular release of ATP and HMGB1, and by monitoring cell surface levels of the immune-activating protein calreticulin (33). In U-2OS cells, Dox increased the extracellular release of LDH (Fig. 1F), ATP (Fig. 1G) and HMGB1 (Fig. 1H), and surface expression of calreticulin (Fig. 1I), but it progressively lost these properties in the resistant variants. By contrast, mtDox increased all these parameters in sensitive and resistant cells (Fig. 1F–I).

The effects of mtDox were not cell line– or species-specific. Indeed, mtDox exhibited greater intracellular accumulation and was more cytotoxic than Dox in human Saos-2 cells and the corresponding resistant variants Saos-2/DX30, Saos-2/DX100, and Saos-2/DX580 cells (Supplementary Fig. S3A and S3B; Supplementary Table S1), as well as in murine Pgp-expressing K7M2 cells (Supplementary Fig. S3C–S3E; Supplementary Table S1). However, mtDox exhibited lower intracellular accumulation (Supplementary Fig. S4A and S4D) and was less toxic (Supplementary Fig. S4B, S4C, S4E, and S4F), in nontransformed osteoblasts and H9c2 cardiomyocytes, where it had a higher IC_{50} than Dox (Supplementary Table S1).

K7M2 tumors implanted in immunocompetent BALB/c mice did not respond to the MTD (5 mg/kg) of Dox (Fig. 2A–C). Dox neither reduced K7M2 cell proliferation (Fig. 2D), nor increased the activity of caspase 3 (Fig. 2E), the amount of surface calreticulin (Fig. 2F), the tumor cell phagocytosis by DCs (Fig. 2G). On the contrary, mtDox elicited all these effects (Fig. 2). Immuhistochemical staining of K7M2 tumor sections confirmed that mtDox reduced tumor cell proliferation, increased apoptotic and calreticulin-positive cells, and increased intratumor infiltration of DCs (Supplementary Fig. S5). According to the hematochemical parameters of the animals at the time of sacrifice, mtDox was significantly less cardiotoxic than Dox and did not elicit liver or kidney toxicity (Table 1). Dose–response experiments revealed that the antitumor effect of mtDox was dose-dependent and that the drug was still effective against resistant osteosarcoma at 1 of 5 of Dox MTD (Supplementary Fig. S6). By contrast, mtDox did not produce any significant advantage compared with Dox against drug-sensitive tumors (Supplementary Fig. S7).

Mitochondria-targeting Dox deeply alters the expression of mitochondria-related genes in Dox-resistant osteosarcoma cells

We next analyzed the expression of genes involved in mitochondria functions and mitochondria-dependent apoptosis. As shown in Fig. 3A and Supplementary Table S2, the progressive increase in Dox resistance was paralleled by the upregulation of genes controlling processing, import, and folding of mitochondrial proteins; mitochondrial fusion, fission, and trafficking; transport of metabolites and cofactors across the mitochondrial membranes; mitochondrial metabolic pathways, such as TCA cycle, fatty acids β-oxidation, and electron transport; ATP synthesis; and ROS protection, such as superoxide dismutase (*SOD*) 1

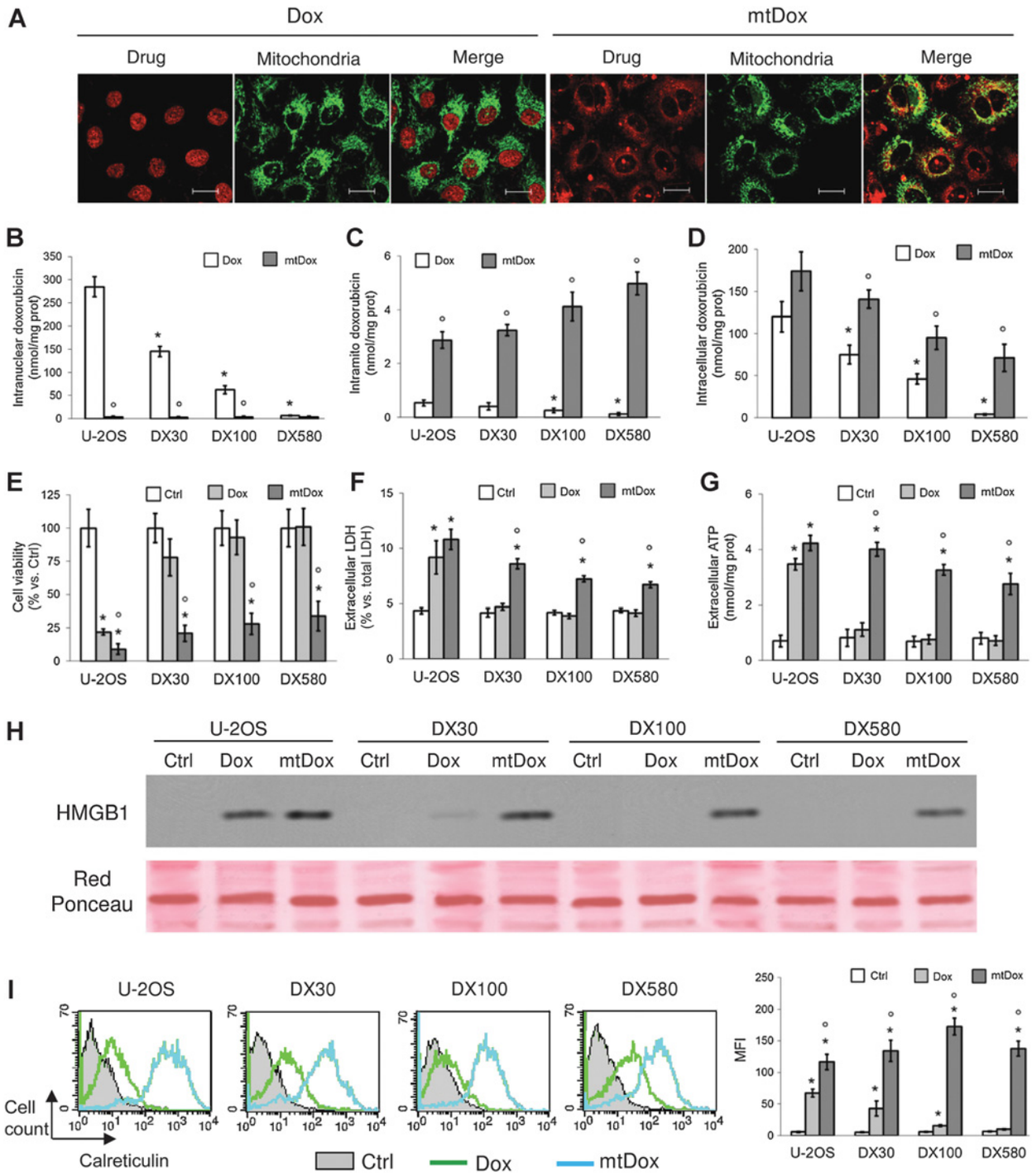

Figure 1.

Mitochondria-targeted Dox is more accumulated and more cytotoxic than Dox in drug-resistant osteosarcoma cells. Dox-sensitive U-2OS cells and Dox-resistant variants (U-2OS/DX30, U-2OS/DX100, U-2OS/DX580) were incubated in the absence (Ctrl) or in the presence of 5 μmol/L Dox or mtDox for 6 hours (**A–D**), 24 hours (**F–I**), or 72 hours (**E**). **A,** U-2OS cells were incubated for 24 hours with the GFP-E1α pyruvate dehydrogenase expression vector to label mitochondria, then treated with Dox or mtDox. The intracellular localization of the drugs was analyzed by confocal microscopy. Bar, 10 μm. The micrographs are representative of 3 experiments with similar results. **B,** the amount of Dox was measured spectrofluorimetrically in nuclear extracts in duplicate. Data are presented as mean ± SD ($n = 3$). Versus U-2OS cells: *, $P < 0.001$; mtDox versus Dox: °, $P < 0.001$. **C,** the amount of Dox was measured spectrofluorimetrically in isolated mitochondria in duplicate. Data are presented as mean ± SD ($n = 3$). Versus U-2OS cells: *, $P < 0.02$; mtDox versus Dox: °, $P < 0.001$. **D,** the content of Dox in whole cell lysates was measured spectrofluorimetrically in duplicate. Data are presented as mean ± SD ($n = 4$). Versus U-2OS cells: *, $P < 0.05$; mtDox versus Dox: °, $P < 0.002$. **E,** cells were stained with neutral red solution in quadruplicate. (*Continued on the following page.*)

and 2. However, genes encoding for proteins uncoupling oxidative phosphorylation and ATP synthesis, such as *SLC25A27* and *UCP1*, were progressively downregulated.

In drug-sensitive U-2OS cells, both Dox and mtDox downregulated at least 2-fold 25 genes encoding for metabolite transporters, subunits of respiratory chain complexes and ATP synthase, antioxidant genes such as *SOD1* and *SOD2*, and anti-apoptotic genes such as *BCL2* and *BCL2L1* (also known as *Bcl-xL*). They both upregulated genes encoding for the uncoupling proteins SLC25A27, UCP1, UCP2, UCP3 as well as the pro-apoptotic genes *BAK1*, *BBC3* (also known as *PUMA*), and *BNIP3* (Fig. 3B; Supplementary Table S3). In U-2OS/DX580 cells, Dox up- or downregulated most of these genes less than 1-fold, consistently with the low-drug accumulation and efficacy. MtDox, by contrast, downregulated at least 2-fold the vast majority of genes involved in protein import and processing, mitochondrial fusion and fission, metabolite and electron transport, ATP synthesis, ROS protection, and apoptosis inhibition. In parallel, mtDox upregulated genes encoding for uncoupling proteins (e.g., *SLC25A27*, *UCP1*, and *UCP3*) and proapoptotic factors (e.g., *BAK1*, *BBC3*, *BID*, *BNIP3*; Fig. 3C; Supplementary Table S4).

Given the distinct signatures of drug-sensitive versus drug-resistant variants and the diverse effects of Dox versus mtDox in resistant cells, we then investigated the impact of mtDox on mitochondria biogenesis and energy metabolism in our osteosarcoma models. Up- or downregulation of key mitochondria-related genes was validated by qRT-PCR (Supplementary Tables S5–S7). For the sake of simplicity, we only show the results obtained in U-2OS and U-2OS/DX580 cells. The effects of Dox and mtDox on gene expression and mitochondrial functions of U-2OS/DX30 and U-2OS/DX100 variants were intermediate relative to those produced in U-2OS and U-2OS/DX580 cells.

Mitochondria-targeted Dox reduces mitochondrial biogenesis, protein import, and energy metabolism in Dox-resistant osteosarcoma cells

Compared with U-2OS cells, U-2OS/DX580 cells had higher mitochondrial DNA (Fig. 4A) and protein content (Fig. 4B), a higher level of nuclear translocation of PGC-1α (Fig. 4C), and higher expression of COX-I (Fig. 4D), which is encoded by mitochondrial DNA. These observations are consistent with increased mitochondria biogenesis in the resistant variant. SDH-A, which is encoded by nuclear DNA, was also higher (Fig. 4E), likely in consequence of the higher expression of mitochondrial protein importers in U-2OS/DX580 cells. Consistent with the gene expression signature, U-2OS/DX580 cells had elevated: TCA cycle (Fig. 4F); fatty acids β-oxidation rate (Fig. 4G); ATP-linked OCR (Fig. 4H and I); maximal respiration capacity (Fig. 4H and J), and ATP synthesis by oxidative phosphorylation (Fig. 4K). Dox and mtDox decreased all these parameters in drug-sensitive cells. Only mtDox affected these pathways in drug-resistant cells (Fig. 4).

Mitochondria-targeting Dox triggers a mitochondria-dependent apoptosis in drug-resistant osteosarcoma cells

We did not detect any significant differences in intramitochondrial ROS levels in U-2OS and U-2OS/DX580 cells (Fig. 5A). Dox increased ROS in drug-sensitive cells but not in drug-resistant ones; mtDox significantly increased intramitochondrial ROS in both cell populations (Fig. 5A). The higher levels of ROS were paralleled by mitochondrial depolarization (Fig. 5B). Dox increased proapoptotic proteins such as BAK, active BID (tBID), and PUMA, and decreased antiapoptotic proteins such as BCL-2 and BCL-xL only in U-2OS cells. mtDox elicited these effects in both variants (Fig. 5C), in line with its effects on gene expression. Consistent with the change in mitochondria polarization, Dox increased mitochondria-associated Bad, Bak, Bax, tBid, Bim_L, and Puma, the release of cytochrome c into the cytosol (Fig. 5D), the activity of caspase 9 (Fig. 5E) and caspase 3 (Fig. 5F) only in drug-sensitive cells, whereas mtDox produced these effects in both U-2OS and U-2OS/DX580 cells (Fig. 5D–F).

Discussion

Because targeting mitochondria is an effective therapeutic strategy in osteosarcoma (16), we used chemically modified Dox with a mitochondrial tropism against Dox-sensitive and Dox-resistant osteosarcoma cells. This modified mtDox was effective against osteosarcoma cells overexpressing Pgp and showing resistance to Dox.

The selective delivery into the mitochondria, due to the conjugation of the anthracycline moiety with a peptide containing cationic and hydrophobic residues that deliver cargoes into mitochondria (34), may limit the availability of Dox for the Pgp on the plasma membrane, reducing the efflux of the drug from tumor cells (18). Our work supports this hypothesis. Unlike Dox, mtDox was well retained within mitochondria in both drug-sensitive and drug-resistant/Pgp-overexpressing osteosarcoma cells. Although Dox accumulation and cytotoxic efficacy dramatically decreased in the Pgp-overexpressing variants, mtDox accumulation within resistant cells was only slightly lower, and its cytotoxicity remained high in Pgp-overexpressing cells. Although these data might suggest that Pgp effluxes both mtDox and Dox, the preferential intramitochondrial delivery of the former preserves its high intracellular retention.

The higher the intracellular accumulation of Dox, the higher the ability of the drug to kill cancer cells due to the induction of necro-apoptotic death and activation of the host immune system against the tumor (35): Dox promotes the exposure on the plasma membrane of calreticulin, which activates the local DCs to phagocytize tumor cells, stimulating a subsequent

(*Continued.*)The results were expressed as a percentage of viable cells versus untreated cells. Data are presented as mean ± SD ($n = 3$). Versus respective Ctrl: *, $P < 0.001$; mtDox versus Dox: °, $P < 0.01$. **F,** the release of LDH in the extracellular medium was measured spectrophotometrically in duplicate. Data are presented as mean ± SD ($n = 4$). Versus respective Ctrl: *, $P < 0.005$; mtDox versus Dox: °, $P < 0.001$. **G,** the extracellular release of ATP was measured in duplicate by a chemiluminescence-based assay. Data are presented as mean ± SD ($n = 3$). Versus respective Ctrl: *, $P < 0.001$; mtDox versus Dox: °, $P < 0.001$. **H,** the release of HMGB1 in the cell supernatants was analyzed by Western blotting. Red Ponceau staining was used to check the equal loading of proteins. The figure is representative of 1 of 3 experiments. **I,** the amount of surface calreticulin was measured by flow cytometry in duplicate. Left, histograms representative of 3 experiments with similar results; right: mean fluorescence intensity (MFI) of calreticulin-positive cells. Data are presented as mean ± SD ($n = 3$). Versus respective Ctrl: *, $P < 0.01$; mtDox versus Dox: °, $P < 0.001$.

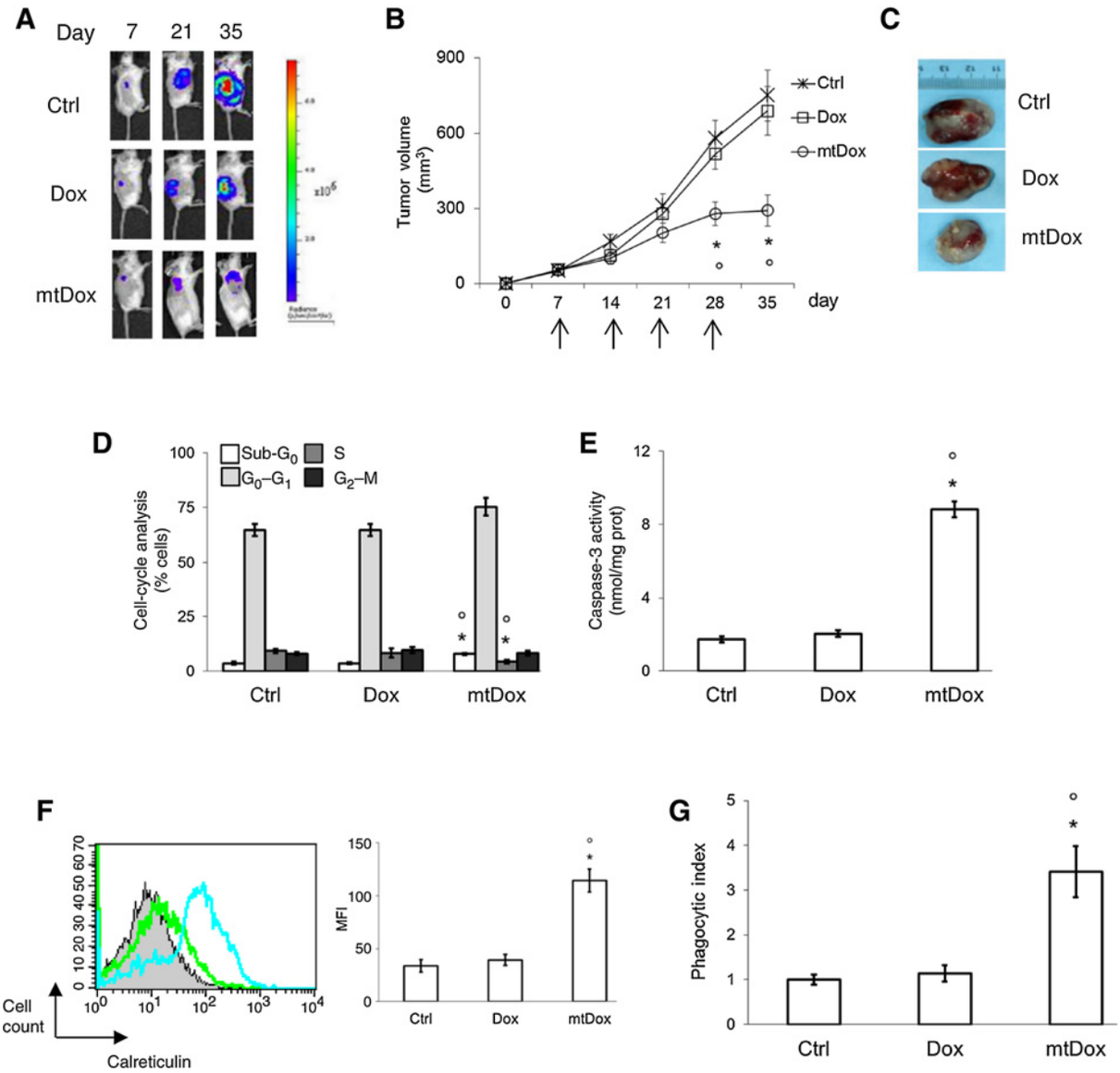

Figure 2.

Mitochondria-targeted Dox is effective against drug-resistant osteosarcoma *in vivo*. Six-week-old female BALB/c mice were inoculated s.c. with 1×10^6 K7M2 cells. When the tumor reached the volume of 50 mm^3 (day 7), the animals (10 mice/group) were randomized and treated on days 7, 14, 21, and 28 as follows: (1) Ctrl group, treated with 0.1 mL saline solution i.v.; (2) Dox group, treated with 5 mg/kg Dox i.v.; (3) mtDox group, treated with 5 mg/kg mitochondria-targeted Dox i.v. **A,** representative *in vivo* bioluminescence imaging, performed on days 7, 21, and 35 after implant. **B,** tumor growth monitored by caliper measurements. Arrows represent saline, Dox, or mtDox injections. Data are presented as mean ± SD. Versus Ctrl group: *, $P < 0.001$; mtDox group versus Dox group: °, $P < 0.001$. The inhibition rate in Dox-treated animals was 16.86%, in mtDox-treated animals, it was 45.49%. **C,** photographs of representative tumors from each treatment group after mice sacrifice. **D–G,** K7M2 cells were left untreated (Ctrl) or treated for 24 hours with 5 μmol/L Dox or mtDox. **D,** cell-cycle analysis was measured by flow cytometry. Data are presented as mean ± SD ($n = 3$). Versus Ctrl: *, $P < 0.01$; mtDox versus Dox: °, $P < 0.001$. **E,** the activity of caspase 3 was measured fluorimetrically in duplicate in the cytosolic extracts. Data are presented as mean ± SD ($n = 4$). Versus Ctrl: *, $P < 0.001$; mtDox versus Dox: °, $P < 0.001$. **F,** the amount of surface calreticulin was measured by flow cytometry in duplicate. Left, histograms are representative of 1 of 3 experiments; right, mean fluorescence intensity (MFI) of calreticulin-positive cells. Data are presented as mean ± SD ($n = 3$). Versus Ctrl: *, $P < 0.001$; mtDox versus Dox: °, $P < 0.001$. **G,** DC-mediated phagocytosis of K7M2 cells was measured by flow cytometry. Data are presented as mean ± SD ($n = 4$). The phagocytic index of untreated cells was considered as 1. Versus Ctrl: *, $P < 0.002$; mtDox versus Dox: °, $P < 0.005$.

expansion of antitumor $CD8^+$ T lymphocytes and eliciting a durable antitumor response (36). These mechanisms do not work in drug-resistant tumors (35). Neither cytotoxic nor proimmunogenic effects were exerted by Dox in Pgp-overexpressing osteosarcoma cells. MtDox, however, exerted all the canonical effects of anthracyclines in drug-resistant cells as well, as suggested by the extracellular release of LDH and by the increase of immunogenic cell death biomarkers

Table 1. Hematochemical parameters of animals

	Ctrl	Dox	mtDox
LDH (U/L)	6,231 ± 1,098	6,234 ± 724	6,198 ± 821
AST (U/L)	187 ± 52	234 ± 27	212 ± 82
ALT (U/L)	38 ± 9	41 ± 5	43 ± 10
AP (U/L)	87 ± 13	94 ± 15	91 ± 13
Creatinine (mg/L)	0.041 ± 0.006	0.039 ± 0.008	0.037 ± 0.009
CPK (U/L)	321 ± 93	850 ± 150*	453 ± 83

NOTE: Animals ($n = 10$/group) were treated as reported under Materials and Methods. Blood was collected immediately after mice euthanasia and analyzed for LDH, AST, ALT, AP, creatinine, and CPK. Ctrl, mice treated with saline solution; Dox, mice treated with Dox; mtDox, mice treated with mitochondria-targeting Dox. Versus Ctrl group: $^*P < 0.005$.

(extracellular ATP and HMGB1 release, surface calreticulin). Mitochondrial depolarization, changes in calcium homeostasis, and increased ROS levels have been correlated with calreticulin upregulation and translocation from endoplasmic reticulum (ER) to the plasma membrane (37, 38): indeed, changes in intramitochondrial calcium and ROS are "sensed" by the ER membrane-associated to mitochondria (MAM) compartment, which is rich in calreticulin and controls the protein trafficking to the plasma membrane (39). Because mtDox depolarized mitochondria and increased ROS in both drug-sensitive and drug-resistant osteosarcoma cells, these events likely trigger the upregulation of calreticulin and/or its translocation from ER/MAM to the plasma membrane.

The efficacy of mtDox was validated in a preclinical model of Dox-resistant osteosarcoma implanted in immunocompetent animals, i.e., the Pgp-expressing K7M2 cells that are syngeneic with BALB/c mice. In both *in vitro* and *in vivo* assays, mtDox exerted direct cytotoxicity on tumor cells (as indicated by the reduced tumor growth and cell proliferation, and by the increased apoptosis) and primed tumor cells for the recognition by the host immune system (as suggested by the increased percentage of calreticulin-positive tumor cells, tumor cell phagocytosis, and intratumor DC infiltration). Moreover, mtDox still retained antitumor efficacy at 1/2 to 1/5 of Dox MTD. Importantly, unlike the mice treated with Dox, those treated with mtDox did not show any increase in CPK. These results are in accordance with previous observations, showing that mtDox did not exert systemic and cardio-specific toxicity *in vivo* (19), and with the reduced toxicity observed in cultured cardiomyocytes. In preclinical models, mtDox was more advantageous than Dox in drug-resistant tumors, not in drug-sensitive ones, leading to hypothesize that the greater efficacy of mtDox was due to the targeting of pathways which are crucial for the survival of drug-resistant cells.

The increase of Dox resistance was associated with the upregulation of genes controlling mitochondrial biogenesis, the import of proteins, metabolites and cofactors, and energy metabolism, and with the downregulation of genes encoding for uncoupling proteins. This signature made the mitochondrial metabolism of Dox-resistant osteosarcoma cells more efficient, as confirmed by the higher content of mitochondrial DNA and proteins, and by the higher metabolic flux through the main energy pathways in U-2OS/DX580 cells. It is noteworthy that genes encoded by both nuclear and mitochondrial DNA were upregulated in drug-resistant cells. These results suggest that the higher mitochondrial metabolism of drug-resistant cells was supported partly by the increased mitochondria biogenesis and partly by the increased import of cytosolic proteins and metabolites within mitochondria. This process may favor a more efficient assembly of mitochondrial complexes involved in the TCA cycle, fatty acids β-oxidation, electron transport, and ATP synthesis, and may supply all these pathways with anaplerotic metabolites and essential cofactors. Contrarily to most tumor cells, which obtain energy from anaerobic glycolysis, chemoresistant cells often simultaneously activate glycolysis and oxidative phosphorylation to meet their energy requirements (40). The higher ATP level produced by mitochondrial oxidative phosphorylation may support the ATP-dependent efflux activity of ABC transporters, contributing to the chemoresistant phenotype. On the other hand, a high proton motive force induces a high production of ROS from mitochondria (41). We did not detect any differences in intramitochondrial ROS between U-2OS and U-2OS/DX580 cells, which was most likely due to the upregulation of mitochondrial *SOD2* in the latter: this feature may also contribute to chemoresistance.

Dox acts through pleiotropic mechanisms on tumor cells, including mitochondrial-dependent mechanisms. For example, it reduces the activity of complexes I, II, and III (42) and the synthesis of ATP (43), and increases intramitochondrial ROS through iron-catalyzed redox cycles within complex I (44). In sensitive osteosarcoma cells, Dox downregulated specific metabolite transporters, subunits of mitochondrial respiratory complexes and ATP synthase, cytosolic and mitochondrial isoforms of *SOD*, and upregulated uncoupling proteins and proapoptotic factors. The consequent reduction of mitochondria biogenesis and ATP synthesis, coupled with the increase in intramitochondrial ROS, triggered a mitotoxicity-dependent apoptosis. None of these events occurred in the drug-resistant U-2OS/DX580 variant, where Dox did not reach an intracellular concentration sufficient to elicit effects at genomic and metabolic levels.

By contrast, mtDox produced genomic and metabolic signatures that were similar in drug-sensitive and drug-resistant osteosarcoma cells. By downregulating genes involved in mitochondria biogenesis and mitochondrial protein import, it significantly reduced mitochondrial DNA and protein contents. Previously, it was reported that in cardiomyocytes, mtDox decreased mitochondrial DNA after 6 hours and increased it after 24 hours: This trend suggests a recovery from the initial damage due to mitochondrial biogenesis. On the contrary, in ovarian cancer cells, mitochondrial DNA levels remained significantly lower after 24 hours of treatment with mtDox, indicating that tumor cells are not able to increase mitochondria biogenesis in response to mtDox (19). These findings are in line with the results obtained in osteosarcoma cells. The different response of cardiomyocytes and tumor cells to the mitochondrial damage elicited by mtDox may explain the key properties of mtDox, i.e., its antitumor efficacy and its cardiac safety.

By decreasing the expression of several transporters and subunits of oxidative phosphorylation complexes, mtDox strongly reduced the mitochondrial energy metabolism. It is noteworthy that it upregulated the expression of uncoupling proteins and proapoptotic factors, and markedly decreased the expression of mitochondrial *SOD2*. These events uncoupled oxidative phosphorylation from ATP synthesis and increased the intramitochondrial levels of ROS, which were not buffered by SOD2. This metabolic dysfunction causes the opening of the mitochondrial permeability transition pore and triggers a

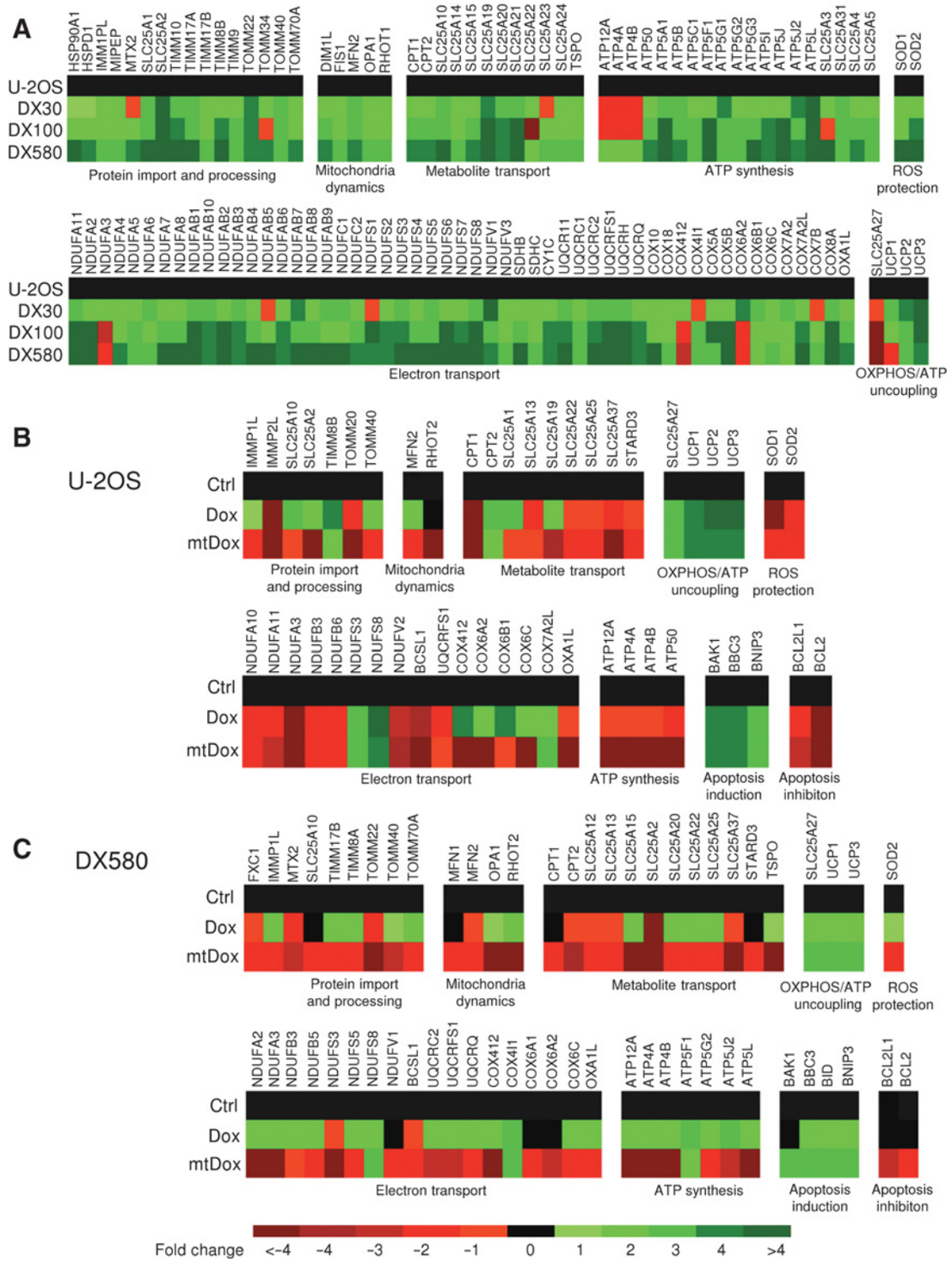

Figure 3.

Modulation of mitochondria-related genes by Dox and mitochondria-targeted Dox in drug-sensitive and drug-resistant osteosarcoma cells. **A,** the cDNA from Dox-sensitive U-2OS cells and Dox-resistant variants (U-2OS/DX30, U-2OS/DX100, and U-2OS/DX580) was analyzed by PCR arrays specific for mitochondria-related genes, as reported under Materials and Methods. The figure reports the genes up- or downregulated 2-fold or more in at least one cell line, in a colorimetric scale ($n = 4$). **B** and **C,** U-2OS cells (**B**) or U-2OS/DX580 cells (**C**) were grown for 24 hours in fresh medium (Ctrl), in medium containing 5 μmol/L Dox, or mtDox. The cDNA was analyzed by the same PCR arrays in **A**. The figures report the genes up- or downregulated 2-fold or more in at least one experimental condition, in a colorimetric scale ($n = 4$). OXPHOS, oxidative phosphorylation.

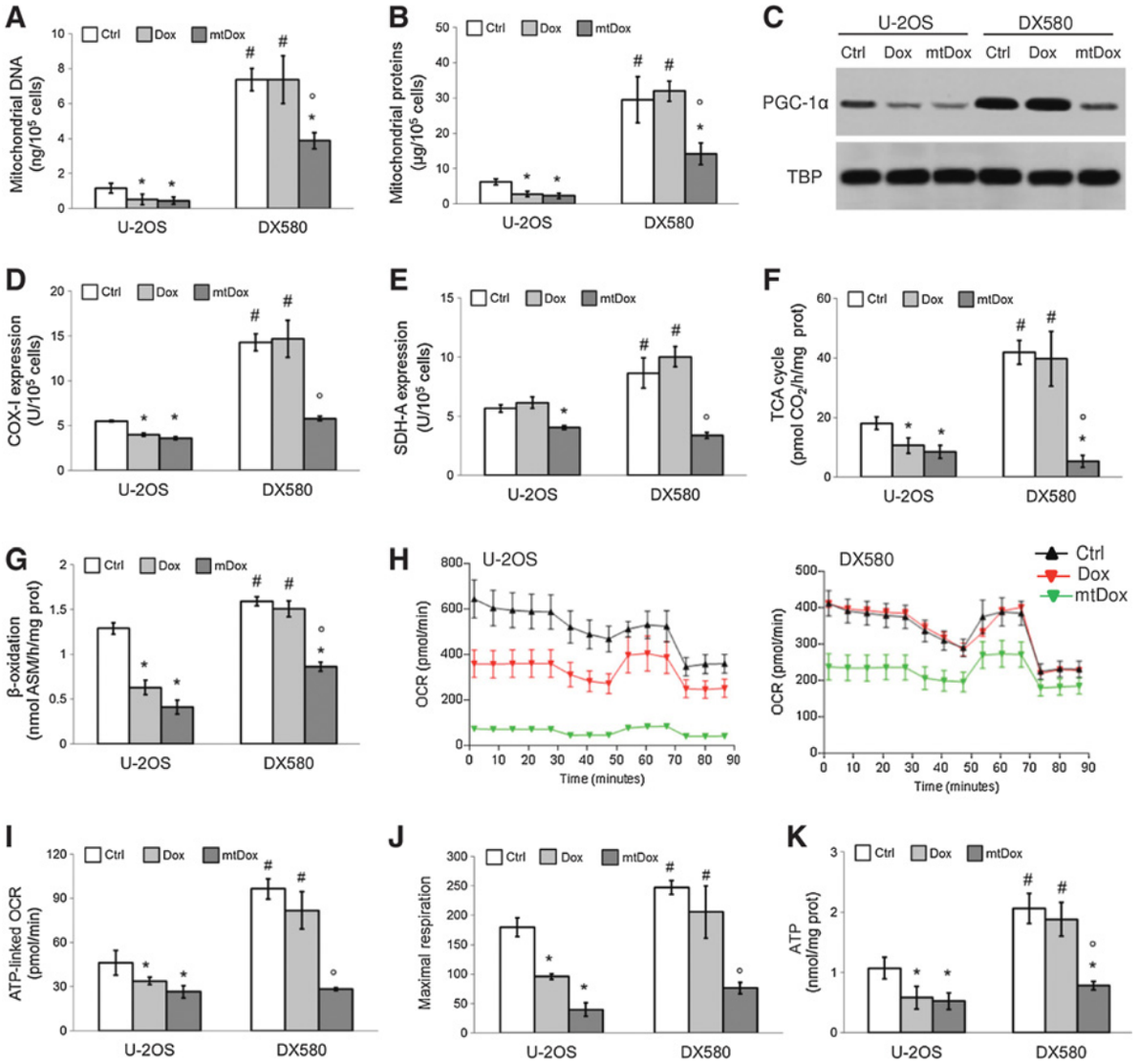

Figure 4.

Mitochondria biogenesis and energy metabolism in cells treated with Dox or mitochondria-targeted Dox. Dox-sensitive U-2OS cells and Dox-resistant U-2OS/DX580 cells were incubated in the absence (Ctrl) or in the presence of 5 μmol/L Dox or mtDox for 24 hours. Data are presented as mean ± SD ($n = 4$). **A** and **B,** the amount of mitochondrial DNA (**A**) and proteins (**B**) was measured in duplicate after mitochondria isolation, as described under Materials and Methods. For both panels, versus U-2OS Ctrl cells: *, $P < 0.05$; versus U-2OS/DX580 Ctrl cells: °, $P < 0.02$; U-2OS/DX580 versus U-2OS cells: #, $P < 0.001$. **C,** nuclear extracts were analyzed for the levels of PGC-1α by Western blotting. The TBP expression was used as the control of equal protein loading. The figure is representative of 1 of 3 experiments. **D** and **E,** the expression of subunit I of complex IV (COX-I, **D**) and succinic acid dehydrogenase-A of complex II (SDH-A, **E**) was measured by quantitative immunocytochemistry in duplicate. For both panels, versus U-2OS Ctrl cells: *, $P < 0.05$; versus U-2OS/DX580 Ctrl cells: °, $P < 0.001$; U-2OS/DX580 versus U-2OS cells: #, $P < 0.05$. **F,** the glucose flux through the TCA cycle was measured in duplicate in cells radiolabeled with [6-^{14}C]-glucose. Versus U-2OS Ctrl cells: *, $P < 0.05$; versus U-2OS/DX580 Ctrl cells: °, $P < 0.001$; U-2OS/DX580 versus U-2OS cells: #, $P < 0.002$. **G,** the amount of ^{14}C-ASM derived from fatty acids β-oxidation was measured in duplicate in cells labeled with [1-^{14}C]-palmitoyl coenzyme A. Versus U-2OS Ctrl cells: *, $P < 0.001$; versus U-2OS/DX580 Ctrl cells: °, $P < 0.001$; U-2OS/DX580 versus U-2OS cells: #, $P < 0.05$. **H,** mitochondrial bioenergetic profiles generated using the Seahorse XFp Analyzer, in U-2OS cells (left) and U-2OS/DX580 cells (right). The figures are representative of 1 of 4 experiments, each performed in triplicate. **I** and **J,** ATP-linked OCR rates (**I**) and maximal respiration (**J**) were determined from the bioenergetic profiles in **H**. ATP-linked OCR represents the difference between basal and oligomycin-treated OCR, whereas maximal respiration represents the difference between FCCP- and rotenone/antimycin-treated OCR. Versus U-2OS Ctrl cells: *, $P < 0.05$; versus U-2OS/DX580 Ctrl cells: °, $P < 0.001$; U-2OS/DX580 versus U-2OS cells: #, $P < 0.05$. **K,** ATP levels in isolated mitochondria were measured in duplicate by a chemiluminescence-based assay. Versus U-2OS Ctrl cells: *, $P < 0.05$; versus U-2OS/DX580 Ctrl cells: °, $P < 0.005$; U-2OS/DX580 versus U-2OS cells: #, $P < 0.01$.

mitochondria-dependent apoptosis. The simultaneous down-regulation of antiapoptotic genes further supported the apoptotic process.

The events described above were more pronounced in Dox-resistant cells than in Dox-sensitive ones, in accordance with the higher mitochondrial metabolic activity of the former. Of note,

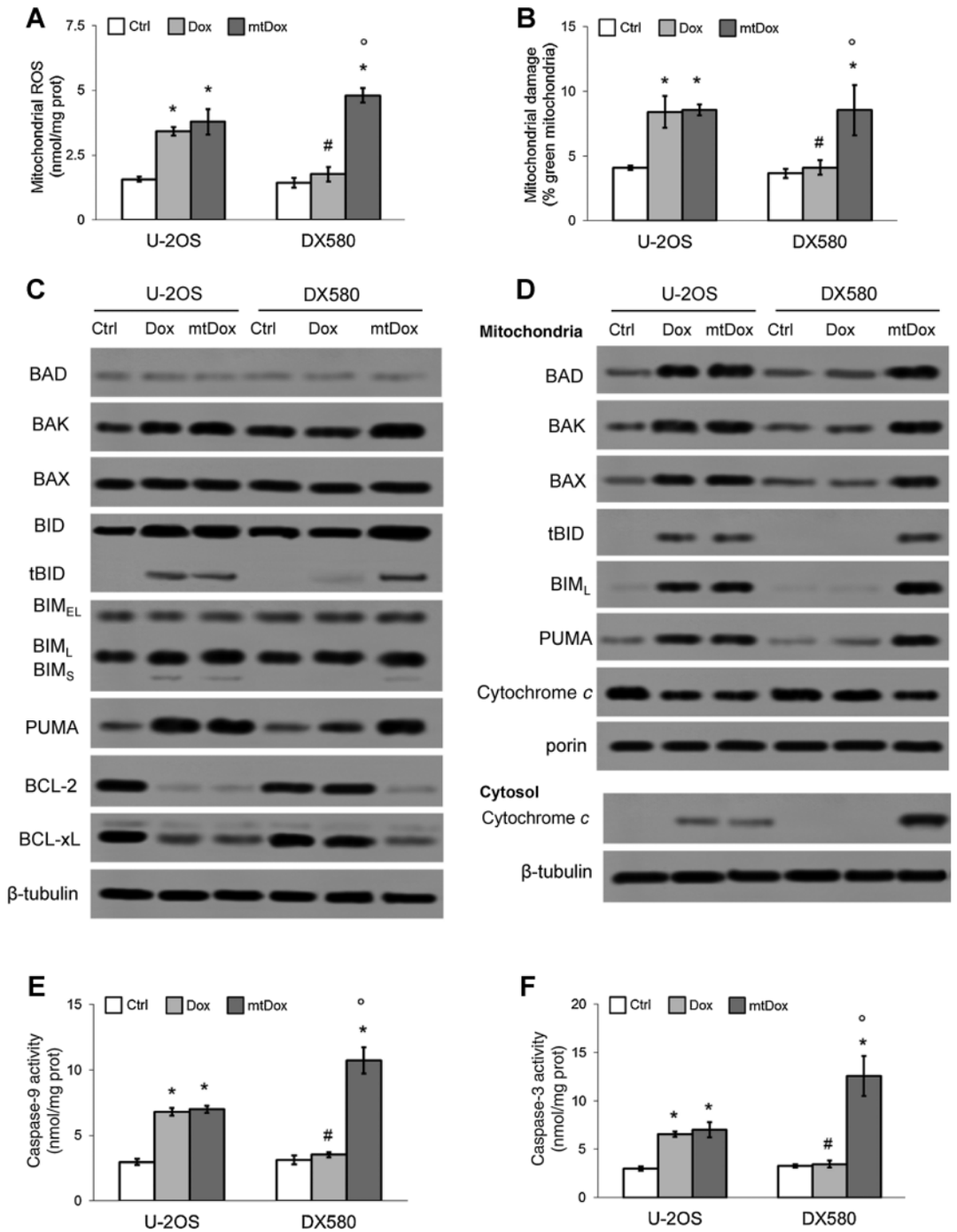

Figure 5.

Effects of Dox and mitochondria-targeted Dox on mitochondria integrity and mitochondria-dependent apoptosis. Dox-sensitive U-2OS cells and Dox-resistant U-2OS/DX580 cells were incubated in the absence (Ctrl) or in the presence of 5 μmol/L Dox or mtDox for 24 hours. **A,** intramitochondrial ROS levels were measured fluorimetrically in triplicate using the DCFDA-AM probe. Data are presented as mean ± SD ($n = 4$). Versus U-2OS Ctrl cells: *, $P < 0.001$; versus U-2OS/DX580 Ctrl cells: °, $P < 0.001$; U-2OS/DX580 versus U-2OS cells: #, $P < 0.001$. **B,** the mitochondrial membrane potential was assessed in duplicate by the JC-1 staining method. The percentage of green versus red mitochondria was considered an index of mitochondrial depolarization and permeability transition. Data are presented as mean ± SD ($n = 4$). Versus U-2OS Ctrl cells: *, $P < 0.005$; versus U-2OS/DX580 Ctrl cells: °, $P < 0.005$; U-2OS/DX580 versus U-2OS cells: #, $P < 0.002$. **C,** whole cell lysates were probed with the indicated antibodies. BID full-length and truncated (tBID) protein, BIM isoforms BIM$_{EL}$, BIM$_L$, BIM$_S$ are shown. The β-tubulin expression was used as the control of equal protein loading. The figure is representative of 1 of 3 experiments. **D,** mitochondrial and cytosolic extracts were subjected to Western blotting and probed with the indicated antibodies. tBID and BIM$_L$ isoforms are shown. Porin and β-tubulin expression were used as the control of equal protein loading in the respective extracts. The figure is representative of 1 of 3 experiments. **E** and **F,** the activity of caspase 9 (**E**) and caspase 3 (**F**) was measured fluorimetrically in duplicate in the cytosolic extracts. Data are presented as mean ± SD ($n = 4$). For both panels, versus U-2OS Ctrl cells: *, $P < 0.001$; versus U-2OS/DX580 Ctrl cells: °, $P < 0.001$; U-2OS/DX580 versus U-2OS cells: #, $P < 0.001$.

mtDox was relatively nontoxic in nontransformed osteoblasts. On the one hand, the lower uptake of mtDox by nontransformed cells may explain the reduced toxicity; on the other hand, osteoblasts are more dependent on anaerobic glycolysis than on mitochondrial metabolism for their growth and differentiation (45, 46). These factors may explain the relatively selective cytotoxicity of mtDox for tumor cells over nontransformed cells.

Despite their resistance to chemotherapy, drug-resistant tumors are more susceptible than drug-sensitive ones to the depletion of ATP and to the increase of ROS, an event known as "collateral sensitivity" (CS; ref. 47). Agents that lower intracellular ATP and/or increase ROS levels are effective against chemoresistant cells *in vitro*. Unfortunately, the intrinsic toxicity of these agents limits their use *in vivo* (48). However, thanks to its ability to lower the levels of ATP produced by oxidative phosphorylation and increase ROS levels within drug-resistant cells, mtDox is an excellent inducer of CS. Unlike the other compounds exerting CS, it did not produce appreciable toxicity for the liver, kidneys, or heart in our preclinical model of resistant osteosarcoma, thus appearing suitable for being used *in vivo*.

The novelty of the therapeutic strategy proposed in this work relates to two factors. First, we used a derivative of the first-line drug Dox, the efficacy of which is limited by the expression of Pgp in osteosarcoma cells and by the development of cardiotoxicity: by chemically modifying Dox to achieve its selective delivery into mitochondria, we overcame a key limitation frequently encountered in patients treated with Dox-based regimens. Second, mtDox exploited a metabolic signature typical of chemoresistant cells—i.e., the hyperactive mitochondrial metabolism—and hit energy pathways that are crucial for drug-resistant tumors. This drug conjugate produced promising results that may be applied to the treatment of Pgp-expressing osteosarcomas. These results may pave the way for the potential use of mtDox in clinical settings, in particular for patients with Pgp-positive osteosarcomas or as a possible second-line treatment for relapsed patients.

Disclosure of Potential Conflicts of Interest

No potential conflicts of interest were disclosed.

Authors' Contributions

Conception and design: S.R. Jean, C. Riganti
Development of methodology: I. Buondonno, V. Audrito, J. Kopecka, C. Costamagna, I. Roato, E. Mungo, S. Deaglio
Acquisition of data (provided animals, acquired and managed patients, provided facilities, etc.): I. Buondonno, E. Gazzano, I.C. Salaroglio, E. Mungo
Analysis and interpretation of data (e.g., statistical analysis, biostatistics, computational analysis): I. Buondonno, E. Gazzano, V. Audrito, J. Kopecka, I.C. Salaroglio, C. Costamagna, S. Deaglio, S.O. Kelley, C. Riganti
Writing, review, and/or revision of the manuscript: I. Buondonno, E. Gazzano, S.R. Jean, M. Fanelli, C.M. Hattinger, S.O. Kelley, M. Serra, C. Riganti
Administrative, technical, or material support (i.e., reporting or organizing data, constructing databases): M. Fanelli, C.M. Hattinger, M. Serra
Study supervision: C. Riganti
Other (synthesized and characterized mitochondria-targeted doxorubicin for the study): S.R. Jean
Other (bioenergetic studies): V. Audrito

Acknowledgments

The authors are grateful to Professor Amalia Bosia, Department of Oncology, University of Torino, for the fruitful discussion, and to Dr. Erika Ortolan, Department of Medical Sciences, University of Torino, for technical assistance. We are also grateful to Mr. Andrew Martin Garvey, BAHons LTCL(TESOL) PGDip MA, for editorial assistance.

Grant Support

This work was supported with funds from Italian Association for Cancer Research (IG15232 to C. Riganti) and Italian Ministry of University and Research (FIRB 2012, grant RBFR12SOQ1 to C. Riganti); Canadian Institutes for Health Research Operating Grant (to S.O. Kelley); 5‰ contributions to Rizzoli Institute (to M. Serra). I. Buondonno and I.C. Salaroglio are recipients of PhD scholarships from the Italian Institute for Social Security (INPS). E. Gazzano is recipient of a postdoctoral fellowship from the Italian Ministry of University and Research. V. Audrito is recipient of the #15047 fellowship from the Italian Association for Cancer Research/Italian Foundation for Cancer Research (FIRC). J. Kopecka is recipient of a fellowship from "Fondazione Umberto Veronesi."

The costs of publication of this article were defrayed in part by the payment of page charges. This article must therefore be hereby marked *advertisement* in accordance with 18 U.S.C. Section 1734 solely to indicate this fact.

Received February 1, 2016; revised June 10, 2016; accepted June 23, 2016; published OnlineFirst July 27, 2016.

References

1. Rivera-Valentin RK, Zhu L, Hughes DP. Bone sarcomas in pediatrics: Progress in our understanding of tumor biology and implications for therapy. Paediatr Drugs 2015;17:257–71.
2. Hattinger CM, Fanelli M, Tavanti E, Vella S, Ferrari S, Picci P, et al. Advances in emerging drugs for osteosarcoma. Expert Opin Emerg Drugs 2015; 20:495–514.
3. Lipshultz SE, Karnik R, Sambatakos P, Franco VI, Ross SW, Miller TL. Anthracycline-related cardiotoxicity in childhood cancer survivors. Curr Opin Cardiol 2014;29:103–12.
4. Gottesman MM, Fojo T, Bates SE. Multidrug resistance in cancer: Role of ATP-dependent transporters. Nat Rev Cancer 2002;2:48–58.
5. Baldini N, Scotlandi K, Barbanti-Bròdano G, Manara MC, Maurici D, Bacci G, et al. Expression of P-glycoprotein in high-grade osteosarcomas in relation to clinical outcome. N Engl J Med 1995;333: 1380–5.
6. Serra M, Scotlandi K, Reverter-Branchat G, Ferrari S, Manara MC, Benini S, et al. Value of P-glycoprotein and clinicopathologic factors as the basis for new treatment strategies in high-grade osteosarcoma of the extremities. J Clin Oncol 2003;21:536–42.
7. Serra M, Pasello M, Manara MC, Scotlandi K, Ferrari S, Bertoni F, et al. May P-glycoprotein status be used to stratify high-grade osteosarcoma patients? Results from the Italian/Scandinavian Sarcoma Group 1 treatment protocol. Int J Oncol 2006;29:1459–68.
8. Bramer JA, van Linge JH, Grimer RJ, Scholten RJ. Prognostic factors in localized extremity osteosarcoma: A systematic review. Eur J Surg Oncol 2009;35:1030–6.
9. Condello M, Cosentino D, Corinti S, Di Felice G, Multari G, Gallo FR, et al. Voacamine modulates the sensitivity to doxorubicin of resistant osteosarcoma and melanoma cells and does not induce toxicity in normal fibroblasts. J Nat Prod 2014;77:855–62.
10. Xia YZ, Ni K, Guo C, Zhang C, Geng YD, Wang ZD, et al. Alopecurone B reverses doxorubicin-resistant human osteosarcoma cell line by inhibiting P-glycoprotein and NF-kappa B signaling. Phytomedicine 2015;22: 344–51.
11. Duan Z, Zhang J, Ye S, Shen J, Choy E, Cote G, et al. A-770041 reverses paclitaxel and doxorubicin resistance in osteosarcoma cells. BMC Cancer 2014;14:e681.
12. Yang X, Yang P, Shen J, Osaka E, Choy E, Cote G, et al. Prevention of multidrug resistance (MDR) in osteosarcoma by NSC23925. Br J Cancer 2014;110:2896–904.
13. Susa M, Iyer AK, Ryu K, Choy E, Hornicek FJ, Mankin H, et al. Inhibition of ABCB1 (MDR1) expression by an siRNA nanoparticulate delivery

system to overcome drug resistance in osteosarcoma. PLoS One 2010;5: e10764.
14. Roncuzzi L, Pancotti F, Baldini N. Involvement of HIF-1α activation in the doxorubicin resistance of human osteosarcoma cells. Oncol Rep 2014; 32:389–94.
15. Sero V, Tavanti E, Vella S, Hattinger CM, Fanelli M, Michelacci F, et al. Targeting polo-like kinase 1 by NMS-P937 in osteosarcoma cell lines inhibits tumor cell growth and partially overcomes drug resistance. Invest New Drugs 2014;32:1167–80.
16. Armstrong J, Dass CR. Doxorubicin action on mitochondria: relevance to osteosarcoma therapy? Curr Drug Targets 2015 Apr 16. [Epub ahead of print].
17. Riganti C, Rolando B, Kopecka J, Campia I, Chegaev K, Lazzarato L, et al. Mitochondrial-targeting nitrooxy-doxorubicin: A new approach to overcome drug resistance. Mol Pharm 2013;10:161–74.
18. Chamberlain GR, Tulumello DV, Kelley SO. Targeted delivery of doxorubicin to mitochondria. ACS Chem Biol 2013;8:1389–95.
19. Jean SR, Tulumello DV, Riganti C, Liyanage SU, Schimmer AD, Kelley SO. Mitochondrial targeting of doxorubicin eliminates nuclear effects associated with cardiotoxicity. ACS Chem Biol 2015;10:2007–15.
20. Serra M, Scotlandi K, Manara MC, Maurici D, Lollini PL, De Giovanni C, et al. Establishment and characterization of multidrug-resistant human osteosarcoma cell lines. Anticancer Res 1993;13:323–9.
21. Gronthos S, Zannettino AC, Hay SJ, Shi S, Graves SE, Kortesidis A, et al. Molecular and cellular characterisation of highly purified stromal stem cells derived from human bone marrow. J Cell Sci 2003;116:1827–35.
22. Brunetti G, Rizzi R, Oranger A, Gigante I, Mori G, Taurino G, et al. LIGHT/TNFSF14 increases osteoclastogenesis and decreases osteoblastogenesis in multiple myeloma-bone disease. Oncotarget 2014;5:12950–67.
23. Gelsomino G, Corsetto PA, Campia I, Montorfano G, Kopecka J, Castella B, et al. Omega 3 fatty acids chemosensitize multidrug resistant colon cancer cells by downregulating cholesterol synthesis and altering detergent resistant membranes composition. Mol Cancer 2013;12:e137.
24. Riganti C, Salaroglio IC, Caldera V, Campia I, Kopecka J, Mellai M, et al. Temozolomide downregulates P-glycoprotein expression in glioblastoma stem cells by interfering with the Wnt3a/GSK3/β-catenin pathway. Neuro-Oncol 2013;15:1502–17.
25. Campia I, Lussiana C, Pescarmona G, Ghigo D, Bosia A, Riganti C. Geranylgeraniol prevents the cytotoxic effects of mevastatin in THP-1 cells, without decreasing the beneficial effects on cholesterol synthesis. Br J Pharmacol 2009;158:1777–86.
26. Riganti C, Miraglia E, Viarisio D, Costamagna C, Pescarmona G, Ghigo D, et al. Nitric oxide reverts the resistance to doxorubicin in human colon cancer cells by inhibiting the drug efflux. Cancer Res 2005;65:516–25.
27. Riganti C, Castella B, Kopecka J, Campia I, Coscia M, Pescarmona G, et al. Zoledronic acid restores doxorubicin chemosensitivity and immunogenic cell death in multidrug-resistant human cancer cells. PLoS One 2013;8: e60975.
28. Obeid M, Tesniere A, Ghiringhelli F, Fimia GM, Apetoh L, Perfettini JL, et al. Calreticulin exposure dictates the immunogenicity of cancer cell death. Nat Med 2007;13:54–61.
29. LeBleu VS, O'Connell JT, Gonzalez Herrera KN, Wikman H, Pantel K, Haigis MC, et al. PGC-1α mediates mitochondrial biogenesis and oxidative phosphorylation in cancer cells to promote metastasis. Nat Cell Biol 2014;16:992–1003.
30. Riganti C, Gazzano E, Polimeni M, Costamagna C, Bosia A, Ghigo D. Diphenyleneiodonium inhibits the cell redox metabolism and induces oxidative stress. J Biol Chem 2004;279:47726–31.
31. Gaster M, Rustan AC, Aas V, Beck-Nielsen H. Reduced lipid oxidation in skeletal muscle from type 2 diabetic subjects may be of genetic origin evidence from cultured myotubes. Diabetes 2004;53:542–8.
32. Riganti C, Gazzano E, Gulino GR, Volante M, Ghigo D, Kopecka J. Two repeated low doses of doxorubicin are more effective than a single high dose against tumors overexpressing P-glycoprotein. Cancer Lett 2015;360: 219–26.
33. Kepp O, Senovilla L, Vitale I, Vacchelli E, Adjemian S, Agostinis P, et al. Consensus guidelines for the detection of immunogenic cell death. Oncoimmunology 2014;3:e955691
34. Horton KL, Stewart KM, Foseca SB, Guo Q, Kelley SO. Mitochondria-penetrating peptides. Chem Biol 2008;15:375–82.
35. De Boo S, Kopecka J, Brusa D, Gazzano E, Matera L, Ghigo D, et al. iNOS activity is necessary for the cytotoxic and immunogenic effects of doxorubicin in human colon cancer cells. Mol Cancer 2009;8: e108.
36. Apetoh L, Mignot G, Panaretakis T, Kroemer G, Zitvogel L. Immunogenicity of anthracyclines: Moving towards more personalized medicine. Trends Mol Med 2008;14:141–51.
37. Biswas G, Guha M, Avadhani NG. Mitochondria-to-nucleus stress signaling in mammalian cells: Nature of nuclear gene targets, transcription regulation, and induced resistance to apoptosis. Gene 2005;354: 132–9.
38. Zhang Y, Liu L, Jin L, Yi X, Dang E, Yang Y, et al. Oxidative stress-induced calreticulin expression and translocation: New insights into the destruction of melanocytes. J Invest Dermatol 2014;134:183–91.
39. Poston CN, Krishnan SC, Bazemore-Walker CR. In-depth proteomic analysis of mammalian mitochondria-associated membranes (MAM). J Proteomics 2013;79:219–30.
40. Martinez-Outschoorn UE, Pestell RG, Howell A, Tykocinski ML, Nagajyothi F, Machado FS, et al. Energy transfer in "parasitic" cancer metabolism: mitochondria are the powerhouse and Achilles' heel of tumor cells. Cell Cycle 2011;10:4208–16.
41. Mailloux RJ, Harper ME. Mitochondrial proticity and ROS signaling: Lessons from the uncoupling proteins. Trends Endocrinol Metab 2012; 23:451–8.
42. Marcillat O, Zhang Y, Davies KJ. Oxidative and non-oxidative mechanisms in the inactivation of cardiac mitochondrial electron transport chain components by doxorubicin. Biochem J 1989;259:181–9.
43. Strigun A, Wahrheit J, Niklas J, Heinzle E, Noor F. Doxorubicin increases oxidative metabolism in HL-1 cardiomyocytes as shown by 13C metabolic flux analysis. Toxicol Sci 2012;125:595–606.
44. Simunek T, Sterba M, Popelova O, Adamcova M, Hrdina R, Gersl V. Anthracycline-induced cardiotoxicity: overview of studies examining the roles of oxidative stress and free cellular iron. Pharmacol Rep 2009;61: 154–71.
45. Esen E, Chen J, Karner CM, Okunade AL, Patterson BW, Long F. WNT-LRP5 signaling induces Warburg effect through mTORC2 activation during osteoblast differentiation. Cell Metab 2013;17:745–55.
46. Regan JN, Lim J, Shi Y, Joeng KS, Arbeit JM, Shohet RV, et al. Upregulation of glycolytic metabolism is required for HIF1α-driven bone formation. Proc Natl Acad Sci U S A 2014;111:8673–8.
47. Pluchino KM, Hall MD, Goldsborough AS, Callaghan R, Gottesman MM. Collateral sensitivity as a strategy against cancer multidrug resistance. Drug Resist Updat 2012;15:98–105.
48. Callaghan R, Luk F, Bebawy M. Inhibition of the multidrug resistance P-glycoprotein: time for a change of strategy? Drug Metab Dispos 2014; 42:623–31.